PRECLINICAL STUDY

Surveillance of spontaneous breast cancer metastasis by TRAIL-expressing CD34^{+} cells in a xenograft model

Anna Rossini · Marta Giussani · Arianna Giacomini ·
Carla Guarnotta · Elda Tagliabue ·
Andrea Balsari

Abstract Tumor necrosis factor-related apoptosis-inducing ligand (TRAIL), delivered as a membrane-bound molecule expressed on the surface of adenovirus-transduced CD34^{+} cells (CD34-TRAIL^{+}), was analyzed for its apoptotic activity in vitro on 12 breast cancer cell lines representing estrogen receptor-positive, HER2^{+} and triple-negative (TN) subtypes and for its effect on tumor growth, vascularization, necrosis, and lung metastasis incidence in NOD/SCID mice xenografted with the TN breast cancer line MDA-MB-231. Mesenchymal TN cell lines, which are the richest in putative tumor stem cells among the different breast cancer cell subtypes, were the most susceptible to apoptosis induced by CD34-TRAIL^{+} cells. Indeed, tumor cell "stemness", assessed based on the proportion of CD44^{+}/CD24^{−/low} cells, was significantly correlated with susceptibility to TRAIL. Moreover, in vitro cytotoxicity experiments showed that CD34-TRAIL^{+} cells selectively targeted CD44^{+}/CD24^{−/low} cells. Although in vivo treatment with CD34-TRAIL^{+} cells did not lead to tumor growth inhibition, treated mice revealed significantly larger areas of necrosis associated with damage of tumor vasculature than did control mice. Moreover, lungs from MDA-MD-231 tumor-bearing mice were completely free of metastases at 12 days after the last injection of CD34-TRAIL^{+} cells, whereas metastases were present in all control mouse lungs. An anti-metastatic effect of CD34-TRAIL^{+} cells was also observed in a model of experimental lung metastases. The correlation between in vitro susceptibility to membrane-bound TRAIL and tumor stem cell content, together with CD34-TRAIL[+] cell-induced inhibition of the metastatic process, points to the selective targeting of cancer stem cells by CD34-armed cells and the potential value of such cells in eradicating tumor stem cells before the onset of overt metastases.

Keywords mTRAIL · Metastasis · Triple-negative breast cancer · Cancer stem cells

A. Rossini · A. Balsari (✉)
Dipartimento di Scienze biomediche per la salute, Università di Milano, Via Mangiagalli 31, 20133 Milan, Italy
e-mail: andrea.balsari@unimi.it

M. Giussani · E. Tagliabue · A. Balsari
Molecular Targeting Unit, Department of Experimental Oncology, Fondazione IRCCS, Istituto Nazionale dei Tumori, Via Amadeo 42, 20133 Milan, Italy

A. Giacomini
Medical Oncology, Università di Milano, Milan, Italy

A. Giacomini
Department of Onco/Hematology, Humanitas Clinical and Research Center, Via Manzoni 56, 20089 Rozzano, Milan, Italy

C. Guarnotta
Tumor Immunology Unit, Human Pathology Section, Department of Health Sciences, University of Palermo, 90127, Palermo, Italy

Introduction

In the last years, significant progress has been made in the understanding of the cellular pathways regulating cell death and in therapeutic strategies to promote tumor cell death. Two major apoptotic pathways have been characterized, one of which is activated by changes in mitochondrial

permeability (intrinsic pathway) and the second, triggered by cell surface death receptors engaging specific ligands (extrinsic pathway) [1]. Activation of the death receptor pathway results in recruitment of adaptor molecules and caspase-8 to form the death-inducing signaling complex, thereby inducing caspase-3 activation and apoptosis [2, 3]. Among the ligands that activate the extrinsic pathway, tumor necrosis factor (TNF)-related apoptosis-inducing ligand (TRAIL), a type II transmembrane protein in the TNF superfamily of death receptor ligands [4], is considered a prime candidate for clinical application based on its ability to induce apoptosis in a panel of hematological cancer cell lines and its minimal toxicity to normal human cells [5]. Recently, Carlo-Stella et al. [6] showed that $CD34^+$ cells transduced with adenovirus to express TRAIL as a membrane-bound molecule on the cell surface (CD34-TRAIL$^+$ cells) exert a potent anti-lymphoma activity. Genetically modified $CD34^+$ stem cells represent optimal vehicles for delivering anti-tumor molecules because they are susceptible to adenoviral infection [7] and can migrate from the bloodstream into several tissues, including tumors [8], and because $CD34^+$ cells express adhesion receptors that interact with counter-receptors on endothelial cells in the tumor microenvironment [9–11], where the presence of inflammatory chemoattractants might help to promote efficient tumor targeting of systemically delivered stem cells [12, 13].

To address the potential therapeutic usefulness of CD34-TRAIL$^+$ cells in breast cancer patients and to help identify the breast tumor subtypes likely to benefit clinically from these cells, we analyzed their pro-apoptotic activity and the possible correlation between sensitivity and expression of four death receptors, TRAIL-R1, -R2, -R3, and -R4, in breast carcinoma cell lines representing the genetic heterogeneity present in primary breast cancer. We then analyzed the anti-tumor activity of CD34-TRAIL$^+$ cells in a xenograft model. We found that membrane-bound TRAIL induced significant cell death in several breast cancer cell lines, especially in triple-negative (TN) lines with mesenchymal features, and that sensitivity to CD34-TRAIL$^+$ cells positively correlated with the proportion of cancer stem cells. Moreover, CD34-TRAIL$^+$ cell treatment prevented development of spontaneous lung metastases in mice bearing subcutaneously (s.c.) injected TN breast tumor cells.

Materials and methods

Cell lines and $CD34^+$ cells

Human breast cancer cell lines (obtained from ATCC) were maintained in: RPMI-1640 (MCF-7, MDA-MB-231, SKBr3, T47D, HCC-1937, and ZR-75-1); Dulbecco's modified Eagle's medium (DMEM) (BT-474); Leibowitz L-15 (MDA-

MB-361, MDA-MB-157, MDA-MB-468, and MDA-MB-453); and DMEM-F12 (SUM-159) supplemented with 10 % fetal bovine serum. Culture medium for SUM-159 cells was also supplemented with 5 μg/ml insulin and that of HCC-1937 and ZR-75-1 cells with 1 % sodium pyruvate, 1 % non-essential amino acids, and 1 % HEPES. Cell lines were routinely tested for mycoplasma and cellular contamination or misidentification using STR analysis (DNA analysis).

$CD34^+$ cells were positively selected using the Auto-MACS device (Miltenyi Biotec, Bergisch-Gladbach, Germany, EU) from peripheral blood of consenting donors of allogeneic stem cells undergoing peripheral blood stem cell mobilization with hematopoietic growth factors.

Adenoviral transduction of $CD34^+$ cells

A replication-deficient adenovirus encoding the human TRAIL gene (Ad-TRAIL) expressed from the CMV promoter was generated as described [14] using human TRAIL cDNA purchased from the Riken BioResource Center (Tsukuba, Ibaraki, Japan) [15]. $CD34^+$ cells were plated at 2×10^6/ml in 1 ml of serum-free Iscove's modified Dulbecco's medium (IMDM) containing an appropriate dilution of adenovector stock for a final MOI of 200 plaque-forming units (pfu)/cell. After incubation at 37 °C in 5 % CO_2 for 2 h, cultures were supplemented with 1 ml IMDM plus FBS 20 % and Boo-sterExpress^{TM} reagent (Gene Therapy Systems, San Diego, CA, USA) (final dilution 1:200) and incubated for 18 h, extensively washed in serum-containing medium, and evaluated for transduction efficiency by flow cytometry.

Flow cytometry

For analysis of Ad-TRAIL transduction efficiency of $CD34^+$ cells, cells were incubated with phycoerythrin (PE)-conjugated anti-TRAIL antibody [clone Rik-2; Becton–Dickinson (B-D), San Jose, CA, USA] and allophyc-ocyanin (APC)-conjugated CD34 antibody (B-D). Expression of TRAIL receptors on the surface of all breast cancer cell lines (1×10^6) was examined using PE-anti-TRAIL-R1, -R2 -R3, and -R4 antibodies (R&D Systems, Minneapolis, MN, USA) and the appropriate isotype controls (B-D and R&D Systems). Samples were analyzed on a FACSCalibur flow cytometry system (B-D) using Cell Quest (B-D) software. Expression levels of TRAIL receptors are indicated as the ratio between the mean fluorescence intensity of anti-TRAIL receptor-stained samples and that of isotype control-stained samples.

The content of putative cancer stem cells ($CD44^+$/$CD24^{-/low}$) in the breast cancer cell lines was evaluated in tumor single-cell suspensions (1×10^6) labeled with PE-conjugated CD24 antibody (clone ML-5; B-D), FITC-conjugated CD44 antibody (clone G44-26; B-D) or the

appropriate isotype controls (B-D) according to the manufacturer's instructions. Samples were analyzed by FACSCanto II system (B-D) and analyzed using FlowJo Software (TreeStar Inc., Ashland, OR, USA).

Analysis of CD34-TRAIL$^+$ cell and soluble TRAIL activity in vitro

Tumor cells were left untreated, treated with soluble TRAIL (sTRAIL) (100 ng/ml) (Alexis Corporation, Lausen, Switzerland), or co-cultured with CD34-TRAIL$^+$ cells at 1:1 effector/target cell ratio for 48 h. The percentage of cell death was calculated based on Annexin-V/propidium iodide (PI) double-staining using the Annexin-V-FITC assay (Bender MedSystems, San Bruno, CA, USA). In brief, cells were washed twice with cold PBS, resuspended in binding buffer (10 mM HEPES, 140 mM NaCl, 5 mM CaCl$_2$, pH 7.4), and incubated with Annexin-V-FITC for 10 min at room temperature in the dark. At the end of the incubation, PI was added and cells were immediately analyzed by flow cytometry. Annexin-V/PI double-staining allows the quantitation of apoptotic (Annexin-V$^+$/PI$^-$) and non-apoptotic, i.e., dead cells (Annexin-V$^+$/PI$^+$ plus Annexin-V$^-$/PI$^+$).

In co-culture experiments, the percentages of residual viable CD44$^+$/CD24$^{-/low}$ cells were calculated to evaluate whether the cytotoxic activity of CD34-TRAIL$^+$ cells might selectively target CD44$^+$/CD24$^{-/low}$ putative cancer stem cells. In brief, cells were washed with cold PBS, stained with PE-conjugated CD24 antibody (B-D) and FITC-conjugated CD44 antibody (B-D), and viable cells gated using 7-AAD staining solution (B-D). To exclude CD34-TRAIL$^+$ cells in the estimation of apoptosis and necrosis and of percentages of viable cells, co-cultures were concurrently stained with APC-conjugated anti-CD45 monoclonal antibody (B-D), which labels CD34$^+$ but not tumor cells. Samples were analyzed on a FACSCanto II system (B-D) using FlowJo Software (TreeStar Inc.).

Activity of CD34-TRAIL$^+$ cells in non-obese diabetic/severe combined immunodeficiency (NOD/SCID) mice

Six- to 8-wk-old female NOD/SCID mice (purchased from Charles River, Milano, Italy, EU) were housed in our animal facilities at constant temperature and humidity, with food and water given ad libitum. All animal procedures were approved by the Ethics Committee for Animal Experimentation of the Istituto Nazionale Tumori of Milan according to the United Kingdom Coordinating Committee on Cancer Research guidelines [16]. Two experiments were performed to evaluate the anti-tumor activity of CD34-TRAIL$^+$ cells in mice xenografted with 5×10^6 cells/mouse of MDA-MB-231 cells injected subcutaneously (s.c.) in the right flank. On day 14 after tumor inoculation,

when tumor volume was $\sim$ 50 mm^3, mice were randomly divided into 2 groups (5 per group in experiment 1; 11 per group in experiment 2). In experiment 1, mice were injected intravenously (i.v.) with CD34-TRAIL$^+$ cells (1×10^6 cells/mouse/injection) or PBS on days 14, 17, 21, and 24, while in experiment 2, injections were identical to those in experiment 1 except administered on days 14, 17, 28, and 31. Mice were monitored twice weekly for tumor size and body weight. Tumors were measured with calipers and tumor volume was calculated as: $(D \times d^2)/2$, where D and d represent the longest and shortest diameters, respectively. At 12 days after the last treatment, all mice in experiment 1 and 5 of 11 of each group in experiment 2 were killed. After one week in the remaining 6 mice per group tumors were surgically removed and animals were killed 18 days later. Lungs from mice in experiment 2 were evaluated for the presence of metastases.

The anti-metastatic effect of CD34-TRAIL$^+$ cells was also investigated in an experimental metastasis model. Eight-week-old female NOD/SCID mice were injected i.v. with 1×10^6 MDA-MB-231 cells followed 4 h later by i.v. injection with CD34-TRAIL$^+$ cells (1×10^6 cells/mouse; 4 mice), CD34$^+$ cells (1×10^6 cells/mouse; 4 mice), or PBS (4 mice). At day 31 post-injection, mice were killed and the number of pulmonary metastases was estimated.

Tumor and lung histology and immunohistochemistry

Formalin-fixed, paraffin-embedded tumor nodules were sectioned at 4 μm, dewaxed, hydrated, and stained with hematoxylin and eosin or processed for immunohistochemistry with mouse anti-mouse CD31 antibody (PECAM-1, clone D-11; 1:50, Santa Cruz Biotechnology, CA, USA) after antigen retrieval in 1 mM EDTA at 95 °C for 30 min or with monoclonal mouse anti-human CD45 antibody (clones 2B11 + PD7/26; 1:100, Dako) after antigen retrieval in citrate buffer, pH 6.0, at 95 °C for 6 min.

Tumor necrosis was detected using TdT-mediated dUTP nick-end-labeling (TUNEL) staining (Roche, Milano, Italy, EU) according to the manufacturer's instructions. Positive signals were revealed by 3,3′-diaminobenzidine staining, and tumor sections were counterstained before analysis by light microscopy.

To visualize lung metastases, 4-μm formalin-fixed, paraffin-embedded lung sections were dewaxed, hydrated, and stained with hematoxylin and eosin or processed for immunohistochemistry with mouse anti-human vimentin (clone V9; 1:400, Dako) after antigen retrieval with citrate buffer, pH 6.0, at 95 °C for 6 min. For each mouse, mean number and size of lung metastases were evaluated in 3 microscopic fields (3.0 × 3.0 mm^2) randomly selected in each histological section. Metastases size expressed in μm

was calculated using ImageJ software by determination of the longest diameter using the scale bar as reference.

Analysis of stained sections

After TUNEL staining, tissue sections were acquired at $20 \times$ magnification with an automatic high-resolution scanner (dotSlide System, Olympus, Tokyo, Japan) and grouped according to non-overlapping red, green, and blue (RGB) images in TIFF format (final resolution, 3.125 pixels/μm). Images were analyzed using the open source imaging software ImageJ (http://rsb.info.nih.gov/ij/). Routines for image analysis were coded in ImageJ macro language and executed on RGB images without further treatment. For each experimental condition, three tissue sections from each tumor nodule were analyzed. Images were first treated for noise reduction using a median filter with a 1.5 pixel radius. Necrotic and total tissue areas were examined using different filter values under direct human supervision. Black areas in final binary images were quantified according to pixel counts to obtain a percentage of necrotic areas expressed as: $100 \times$ (necrotic area/total tissue area).

Tumor vasculature was evaluated in CD31-stained sections acquired at $400 \times$ magnification and using Aperio ImageScope v11.1.2.752 at $2 \times$ magnification in vimentin-stained sections.
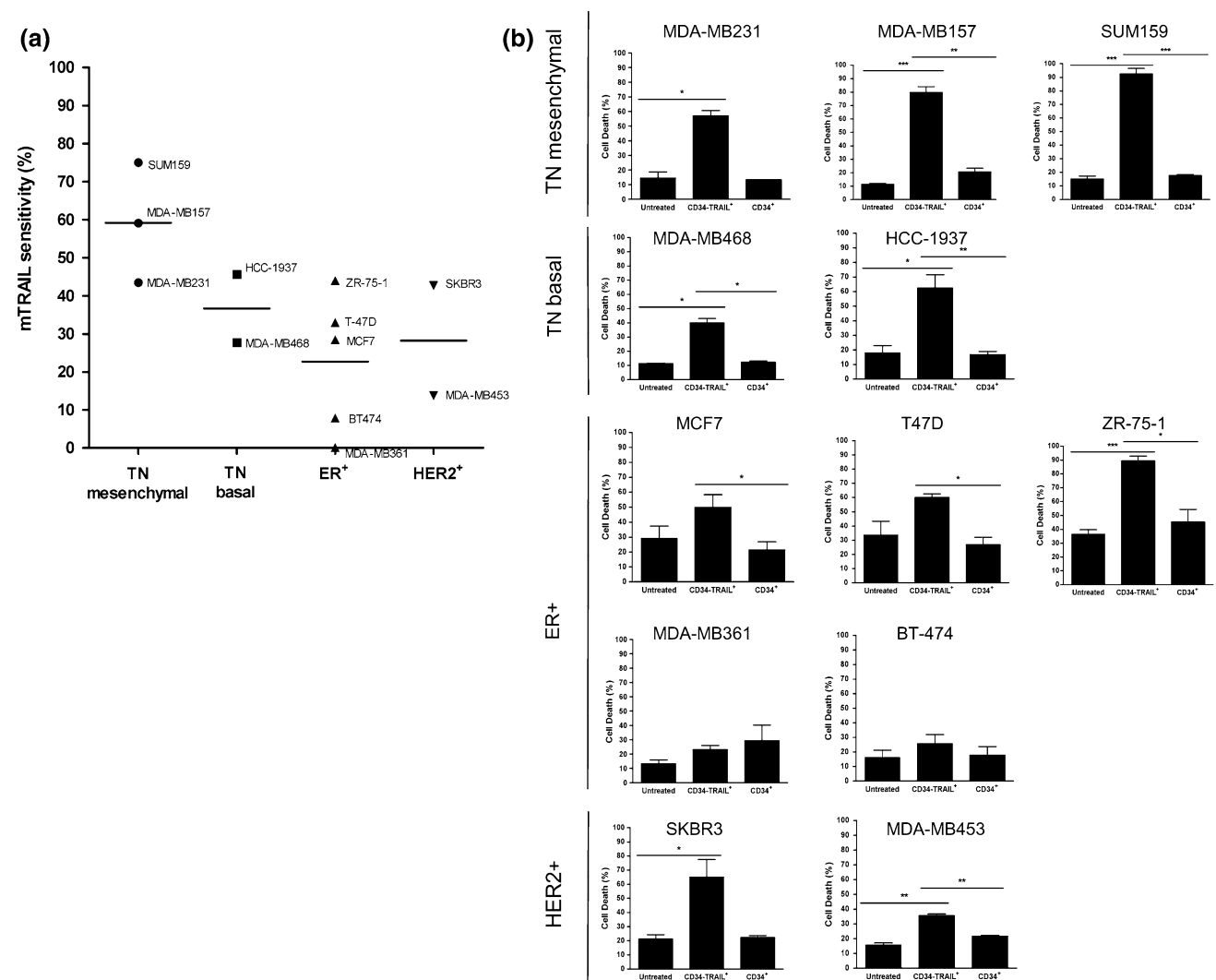

Fig. 1 CD34-TRAIL$^+$ cell-induced toxicity in breast cancer cell lines, Cell lines were incubated with CD34-TRAIL$^+$ or non-transduced CD34$^+$ cells at effector:target cell ratio 1:1 for 48 h, or left untreated. Cell death was measured by flow cytometry to assess Annexin-V/PI labeling. **a** mTRAIL sensitivity, with each cell line grouped according to breast cancer subtype. **b** Cell death of each cell line untreated or after incubation with CD34-TRAIL$^+$ or non-transduced CD34$^+$ cells. *Data* represent mean cell death $\pm$ SEM in three independent experiments with each cell line. Differences between CD34-TRAIL$^+$-treated, non-transduced CD34$^+$-treated and untreated cells were compared by unpaired two-tailed t test. $*P < 0.01$, $**P < 0.001$, $***P < 0.0001$

Statistical analysis

Statistical analysis was performed with the statistical package Prism 5 (GraphPad Software, San Diego, CA, USA). In all in vitro experiments, differences between untreated and treated cells in apoptotic response were analyzed using the unpaired (2-tailed) Student's t test. The correlation between the percentage of CD44$^+$/CD24$^{-/low}$ cells and mTRAIL sensitivity was evaluated by Pearson's Chi-squared test and the correlation between TRAIL receptor expression and mTRAIL sensitivity, by Fisher's exact test. Differences in areas of necrosis and in mean number of lung metastases between the two experimental mouse groups were analyzed using the unpaired (2-tailed) Student's t test. Differences were considered significant at $P \leq 0.05$.

Results

Cell death induced by CD34-TRAIL$^+$ cells in breast cancer cell lines

The cytotoxic activity of CD34-TRAIL$^+$ cells was evaluated in 12 breast cancer cell lines representative of the different breast cancer subtypes classified based on transcriptional profiles as: ER$^+$ (MCF7, ZR-75-1, T47D, BT-474, MDA-MB-361), HER2/neu$^+$ (SKBR3, MDA-MB-453), and mesenchymal (MDA-MB-231, MDA-MB-157, SUM-159) and basal (MDA-MB-468, HCC-1937) TN [17, 18]. These cell lines reflect in some measure the genetic heterogeneity present in primary breast cancer. Remarkable levels of apoptotic cells were observed in most of the cell lines upon co-culture with 1.5×10^5

CD34-TRAIL$^+$ cells at 1:1 effector/target cell ratio (Fig. 1). The percentage of CD34-TRAIL$^+$ cell cytotoxicity, corrected for that of non-transfected CD34$^+$ cells (Fig. 1a), was highest in mesenchymal TN cell lines, ranging from 75 to 43.5 %; in basal TN cell lines, sensitivity ranged from 45.6 to 27.7 %. The apoptotic response in ER$^+$ cell lines was lower than in TN lines and ranged widely (44–0.1 %). In HER2$^+$ cell lines, sensitivity to CD34-TRAIL$^+$ cells ranged from 42.7 to 13.8 %. Breast cancer cell lines co-cultured with non-transduced CD34$^+$ cells showed a similar apoptotic death as untreated cells (Fig. 1b), indicating that the response did not depend on the presence of CD34 per se. Co-culture experiments using one representative cell line for each breast cancer subtype (MDA-MB-231 for mesenchymal triple-negative subtype, MDA-MB-468 for basal triple-negative subtype, ZR-75-1 for ER$^+$ subtype and SKBR3 for HER2$^+$subtype) at increasing effector:target ratios showed that CD34-TRAIL$^+$ cells triggered cell death in a dose-dependent manner (Supplemental Fig. 1), consistent with previous data [6]. Evaluation of the entire panel of breast cancer cell lines for sensitivity to sTRAIL indicated no or only low sensitivity in most cell lines, again consistent with previous results [19]. Supplementary Table 1 reports the comparison between sTRAIL and CD34-TRAIL$^+$ cell cytotoxic activity.

Differential expression of the TRAIL-R1, -R2, -R3, and -R4 receptors on the cell membrane of the cell lines, evaluated in 3 independent experiments, did not appear to account for the differences in sensitivity to mTRAIL, since flow cytometry revealed, with few exceptions, only relatively low-level expression of these death receptors independent of tumor phenotype (Table 1); exceptions included substantial levels of TRAIL-R2 in MDA-MB-231,

Table 1 Expression levels of TRAIL receptors in breast cancer cell lines

Cell line	TRAIL-R1	TRAIL-R2	TRAIL-R3	TRAIL-R4
TN mesenchymal				
MDA-MD-231	1.18 ± 0.07*	3.89 ± 0.84	1.62 ± 0.10	2.25 ± 0.23
MDA-MD-157	1.11 ± 0.03	1.04 ± 0.01	0.99 ± 0.04	1.17 ± 0.03
SUM-159	0.95 ± 0.07	4.70 ± 0.21	1.06 ± 0.07	3.50 ± 0.40
TN basal				
MDA-MD-468	1.07 ± 0.04	1.05 ± 0.03	1.02 ± 0.02	1.05 ± 0.03
HCC-1937	1.08 ± 0.04	1.09 ± 0.04	1.11 ± 0.06	1.04 ± 0.04
ER$^+$ luminal				
ZR-75-1	1.03 ± 0.09	4.48 ± 0.49	3.30 ± 0.37	2.04 ± 0.06
T47D	1.21 ± 0.09	5.42 ± 1.55	2.63 ± 0.51	1.40 ± 0.19
MCF7	1.19 ± 0.10	1.43 ± 0.19	2.09 ± 0.11	1.13 ± 0.01
BT-474	1.07 ± 0.08	1.08 ± 0.08	1.05 ± 0.07	1.03 ± 0.03
MDA-MD-361	0.99 ± 0.06	0.98 ± 0.05	1.09 ± 0.04	0.97 ± 0.05
HER2$^+$				
SKBR3	1.01 ± 0.04	1.09 ± 0.04	1.08 ± 0.04	1.04 ± 0.02
MDA-MD-453	1.19 ± 0.17	1.12 ± 0.08	1.15 ± 0.09	1.08 ± 0.10

* Data are given as mean ± SEM of the ratio between mean fluorescence intensity obtained with specific anti-TRAIL receptor antibodies and that of the corresponding isotype control in 3 independent experiments

SUM-159, T47D, and ZR-75-1 cells, TRAIL-R3 in MCF7, T47D, and ZR-75-1 cells, and TRAIL-R4 in MDA-MB-231, SUM-159, and ZR-75-1 cells. Expression of death-inducing TRAIL-R1, TRAIL-R2, and the antagonistic TRAIL-R3 and TRAIL-R4 did not correlate with sensitivity to CD34-TRAIL^{+} by Fisher's exact test.

"Stemness" and sensitivity to mTRAIL-induced apoptosis

The cell subpopulation expressing cell surface markers CD44^{+}/CD24^{−/low} with increased tumorigenicity has been described as a population enriched in putative cancer stem cells in human breast tumors [20]. Further studies indicated that human breast cancer cell lines with mesenchymal features are enriched in stem cell-like features [21, 22] and recently Rahman et al. [19] demonstrated the strongest sensitivity to sTRAIL by this breast cancer subtype. To test whether the content of putative cancer stem cells was associated with sensitivity to CD34-TRAIL^{+} cells, we first assessed the proportion of CD44^{+}/CD24^{−/low} cells in all cell lines by flow cytometry. Analysis revealed a high proportion of such cells in mesenchymal TN cell lines (94.6 % in MDA-MB-231, 86 % in SUM-159, and 69.5 % in MDA-MB-157), whereas a stem population was low represented in ER^{+}, HER2^{+} or basal TN tumor cell lines, except for the basal TN line HCC-1937, in which CD44^{+}/CD24^{−/low} cells comprised about 29.8 % of cells (Fig. 2a). Pearson's Chi-squared test indicated a significant correlation ($r = 0.7047$, $P = 0.011$) between CD34-TRAIL^{+} cytotoxic activity and the proportion of CD44^{+}/CD24^{−/low}

cells (Fig. 2b). Moreover, in vitro co-culture cytotoxicity experiments using as targets two cell lines with different percentages of CD44^{+}/CD24^{−/low} cells showed that CD34-TRAIL^{+} cells induced a decrease in the percentage of viable CD44^{+}/CD24^{−/low} cells from 94.5 to 63.4 % in MDA-MB-231 cells and from 1 to 0.4 % in SKBR3 cells, indicating the selective cytotoxic activity of CD34-TRAIL^{+} cells. No decrease in CD44^{+}/CD24^{−/low} cells was observed in response to CD34^{+} cells.

Effects of CD34-TRAIL^{+} on MDA-MD-231 subcutaneous xenograft tumors

MDA-MB-231 cells, which were sensitive to mTRAIL in vitro and are able to metastasize spontaneously to lungs [23], were used to evaluate the in vivo effect of CD34-TRAIL^{+} cells. In experiment 1 (Fig. 3, experiment 1), NOD/SCID mice with established s.c. MDA-MB-231 tumors were randomized and inoculated i.v. with CD34-TRAIL^{+} cells (1×10^6 cells/mouse/injection) or PBS on days 14, 17, 21, 24 after tumor cell injection. No significant inhibition of tumor volume was observed in either mouse group (Fig. 3, experiment 1, a). Consistent with a previous finding in a model of hematological tumor [14] that intra-tumor CD34-TRAIL^{+} cells are not detectable beyond 48 h after injection, we found no immunohistochemical staining for the CD45 leukocyte marker indicative of CD34-TRAIL^{+} cells in tumor sections. Nevertheless, TUNEL examination indicated a significant increase in necrotic areas in tumors from CD34-TRAIL[+]-treated versus control mice (19.2 ± 1.7 vs. 9.9 ± 1.0 %; $P = 0.0003$) (Fig. 3,
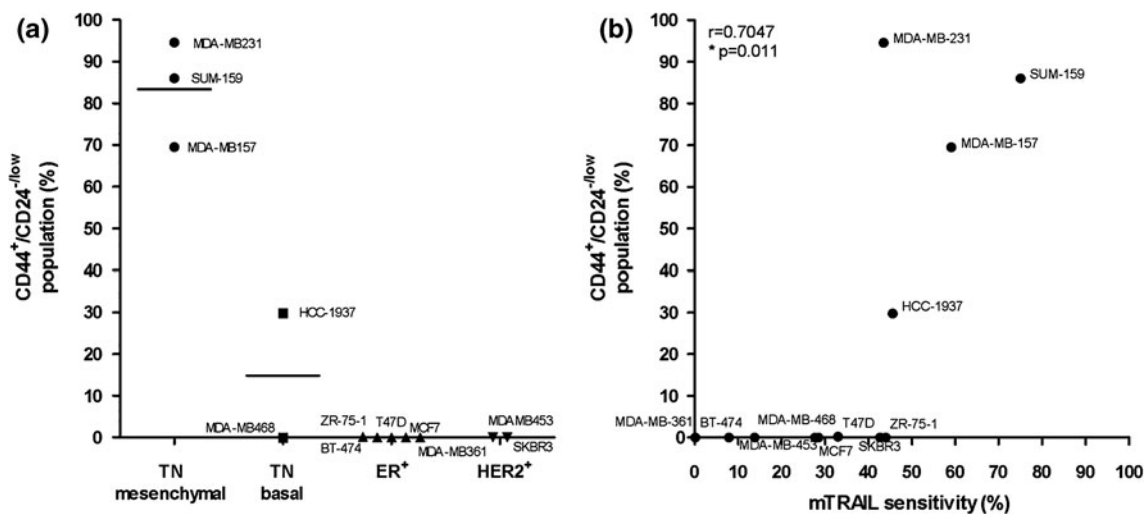

Fig. 2 Correlation between stemness and sensitivity to CD34-TRAIL^{+} cells, **a** content of putative cancer stem cells (percentage of CD44^{+}/CD24^{−/low}) evaluated by flow cytometry. Each *data point* represents the mean percentage of CD44^{+}/CD24^{−/low} in each cell line from three-independent experiments. Cell lines were grouped by

subtype. *Bars* represent the mean percentage of CD44^{+}/CD24^{−/low} for each breast cancer subtype. **b** Correlation analysis between mTRAIL sensitivity and percentage of CD44^{+}/CD24^{−/low} cells using Pearson's Chi-squared test ($P = 0.011$; $r = 0.7047$)
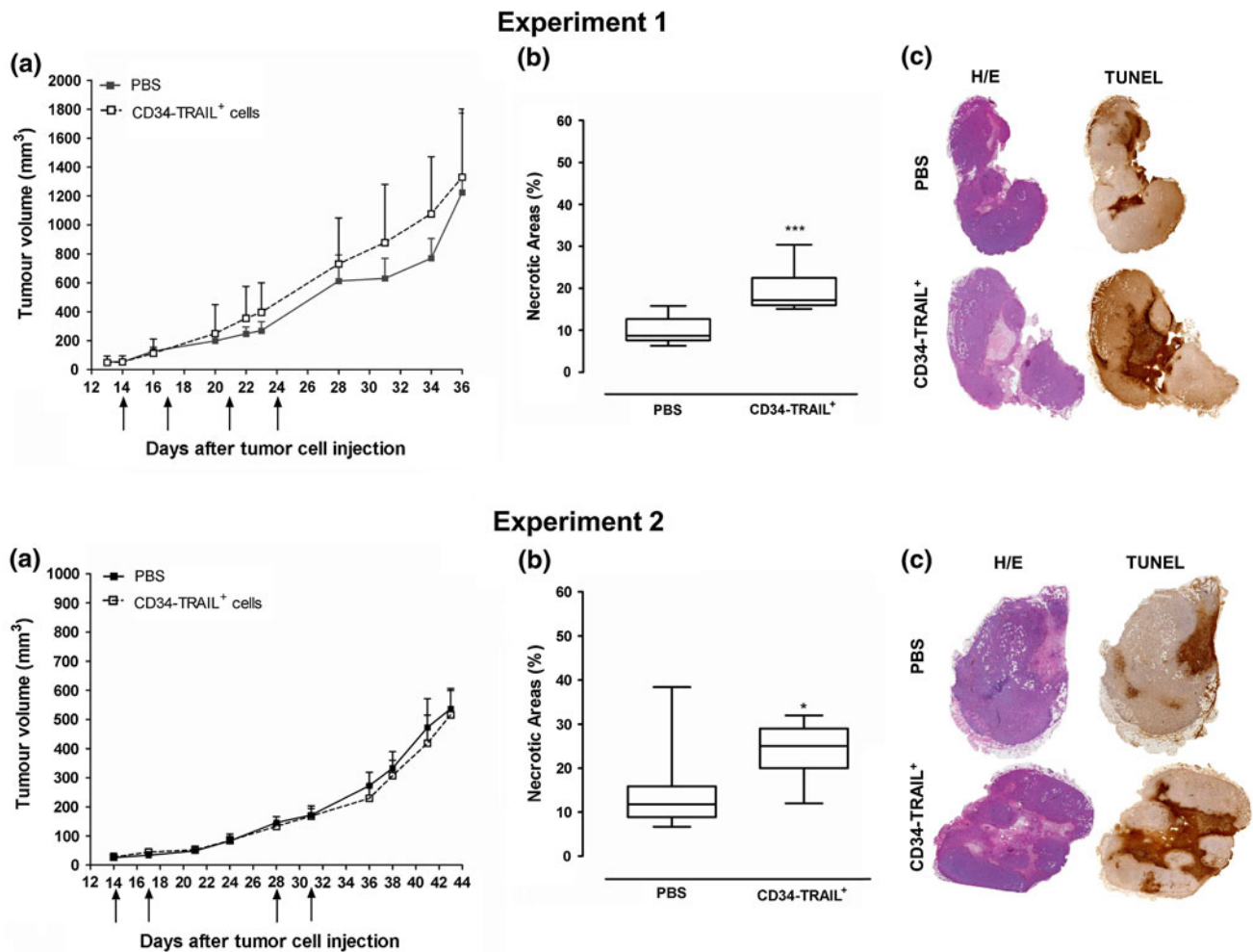
Experiment 1

Experiment 2

Fig. 3 Effects of CD34-TRAIL$^+$ treatment on subcutaneous MDA-MB231 tumors, Experiment 1. **a** Cytotoxic activity of CD34-TRAIL$^+$ cells evaluated in NOD/SCID mice with established s.c. MDA-MB-231 tumors. Mice (5 per group) were treated with PBS (*open square*) or 10^6 CD34-TRAIL$^+$ cells (*filled square*) on days 14, 17, 21, and 24 (*arrows*). Data are given as mean tumor volume ± SD; **b** quantitation of necrotic areas in tumor sections from CD34-TRAIL$^+$- and PBS-treated mice (5 mice/group) labeled for TUNEL assay. Necrotic areas were analyzed using Image J software. Data are given as the ratio of TUNEL-positive areas to total tumor tissue area × 100. *Boxes* extend from the 25th to 75th percentile, *lines* represent the median values, and *whiskers* indicate the range of values. ***$P = 0.0003$ by unpaired two-tailed t test; **c** hematoxylin-eosin and TUNEL staining, revealing more extensive areas of necrosis in tumors of CD34-TRAIL$^+$- as compared to PBS-treated mice. Images for one representative mouse per group are shown. Magnification, × 2. Experiment 2. **a** Same as in experiment 1 except for treatment administration on days 14, 17, 28, and 31 (*arrows*); **b** same as in experiment 1 except for *$P = 0.017$ by unpaired two-tailed t test; **c** same as in experiment 1

experiment 1, b, c). As assessed based on immunohisto-chemical staining for the CD31 endothelial marker, tumors from CD34-TRAIL$^+$-treated mice showed a remarkable decrease in well-structured, branching vessels and a parallel increase in small endothelial sprouts as compared with tumors from PBS-treated mice (Fig. 4). This finding is suggestive of the attempt to rebuild the normal vasculature structure after damage induced upon CD34-TRAIL$^+$ treatment.

To test the effect of CD34-TRAIL$^+$ cells on the metastatic potential of MDA-MB-231 tumors, 22 mice injected s.c. with MDA-MB-231 were randomized into two groups 14 days later and treated i.v. with CD34-TRAIL$^+$ cells

$(1 \times 10^6$ cells/mouse/injection) or PBS on days 14, 17, 28, and 31. Five mice per group were killed 12 days after the last treatment, when tumor volume was about 500 mm^3. Consistent with findings in experiment 1, also in the experiment 2 the necrotic areas in tumors from CD34-TRAIL$^+$-treated mice in experiment 2 were also significantly increased as compared with that in control mice (23.7 ± 1.7 vs. 15.6 ± 1.7 %; $P = 0.017$) (Fig. 3, experiment 2, b, c), without inhibition of tumor growth (Fig. 3, experiment 2, a). These tumors also displayed a picture suggestive of an attempt to restore normal vascular structure after CD34-TRAIL$^+$ treatment (not shown). Analysis of metastases in lung sections stained with vimentin, a
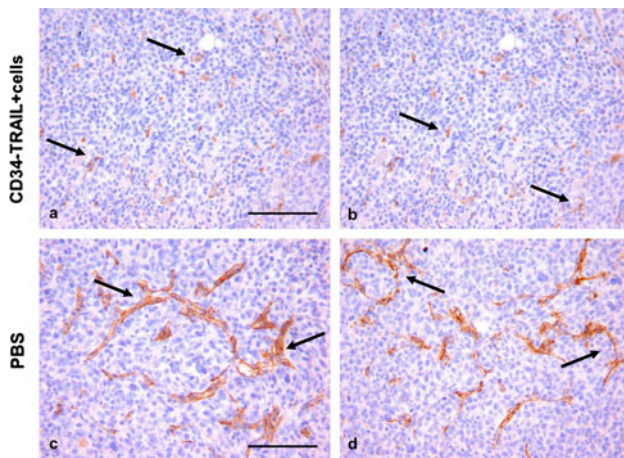
Fig. 4 Effects of CD34-TRAIL$^+$ cell treatment on tumor vasculature, Immunohistochemical analysis of the intra-tumoral vascular network of PBS- and CD34-TRAIL$^+$ cell-treated tumor-bearing mice revealed an abundance of poorly structured microvessels and endothelial sprouts (**a** and **b**, *arrows*) in the tumor vascularity of mTRAIL-treated mice in contrast to the branching vessels characterizing control mice (**c** and **d**, *arrows*). Representative areas of four anti-CD31 immunostained sections are shown. Original magnifications, × 20; *bar* 100 μm; and × 40; *bar* 50 μm

mesenchymal marker highly expressed in MDA-MB-231 cells, revealed 27 ± 22 metastases in the 5 control mice, but no metastases in any of the 5 CD34-TRAIL$^+$ cell-treated mice examined ($P = 0.0079$). One week after metastasis analysis in these 10 mice, s.c. tumors were surgically removed in the remaining 12 mice; 18 days later, mice were killed and lungs were analyzed. The average number of lung metastases was 312 in control mice and 61 in CD34-TRAIL$^+$ cell-treated mice. This difference, although not statistically significant since 1 of the 6 control mice was completely devoid of lung metastases, supports a role for CD34-TRAIL$^+$ cells in the control of the spontaneous metastatic process. Note that metastases in control mouse lungs were $\sim$ 2-fold larger than in CD34-TRAIL$^+$ cell-treated mice, with a mean size of 400 μm in controls versus 200 μm in treated mice (Fig. 5).

In the model of experimental lung metastases, the mean ($\pm$ SD) number of pulmonary metastases in CD34-TRAIL$^+$ cell-treated mice was also lower than in CD34$^+$ cell- and PBS-treated mice (22 ± 6 in CD34$^+$ cell-treated mice, 17 ± 7 in PBS-treated mice, and 3 ± 2 in CD34-TRAIL$^+$ cell-treated mice; $P = 0.0018$ CD34-TRAIL$^+$ cells versus CD34$^+$ cells; $P = 0.018$ CD34-TRAIL$^+$ cells versus PBS).

Discussion

The use of stem and/or progenitor cells as delivery vehicles for therapeutic gene products is emerging as a strategy to improve the efficacy of currently available antitumor therapies. Multiple potential sources of clinically useful stem and progenitor cells have been identified, including autologous and allogeneic embryonic, fetal, and adult somatic cells from neural, adipose and mesenchymal tissues [24–27]. Hematopoietic CD34$^+$ cells, which can be easily mobilized, harvested, enriched, and genetically engineered by adenovector transduction, represent a particularly feasible clinical strategy for systemic TRAIL delivery. Furthermore, hematopoietic CD34$^+$ cells used as vectors of TRAIL delivery reportedly home to or at least engraft preferentially within tumors [14]. The specific mechanisms underlying this tumor tropism of cell-based delivery remain unclear, although it is plausible that different homing signals such as inflammatory chemoattractants and those from cytokines and adhesion molecules present in the tumor microenvironment contribute to tumor-homing of CD34-TRAIL$^+$ cells.

In the present study, we found that CD34-TRAIL$^+$ cells exerted significant cell killing activity in breast cancer cell lines representative of the biological and prognostic heterogeneity of the disease. Target cell death occurred by apoptosis and did not correlate with the levels of death-inducing TRAIL receptor expression. The latter finding is not surprising since many tumors that express high levels of TRAIL-R1 and/or TRAIL-R2 are resistant to soluble TRAIL [28–32]. Among the cell lines examined, the stemness-enriched mesenchymal TN cell lines were the most susceptible to apoptosis induced by CD34-armed cells, and susceptibility to mTRAIL was significantly correlated with stemness. Moreover, cytotoxicity experiments indicated a selective cytotoxic activity of mTRAIL against CD44$^+$/CD24$^{-/low}$ cells. These findings point to the potential usefulness of TRAIL-induced apoptosis in the CD44$^+$/CD24$^{-/low}$ fraction of tumors in overcoming the refractory nature of these putative cancer stem cells to conventional therapy. Indeed, other studies reported that cancer stem cells are sensitive to the TRAIL-mediated cell death pathway [19, 33].

In both of our in vivo experiments, CD34-TRAIL$^+$ cell treatment induced significant necrosis as compared to controls in s.c. growing tumors, but did not interfere with tumor growth. This finding is not readily explained, since proliferation of tumors is thought to depend on the establishment of tumor vasculature to provide nutrients required for cancer cell expansion [34]. In our model, consistent with that described in-depth in an s.c. multiple myeloma model [14], CD34-TRAIL$^+$ cell treatment appeared to induce endothelial damage in the tumor but without the tumor growth inhibition observed in hematological tumors [14]. It is possible that MDA-MB-231 cells overcome the effect of mTRAIL on endothelial cells through the formation of fluid-conducting networks by non-endothelial cells as a result of vasculogenic mimicry, a feature
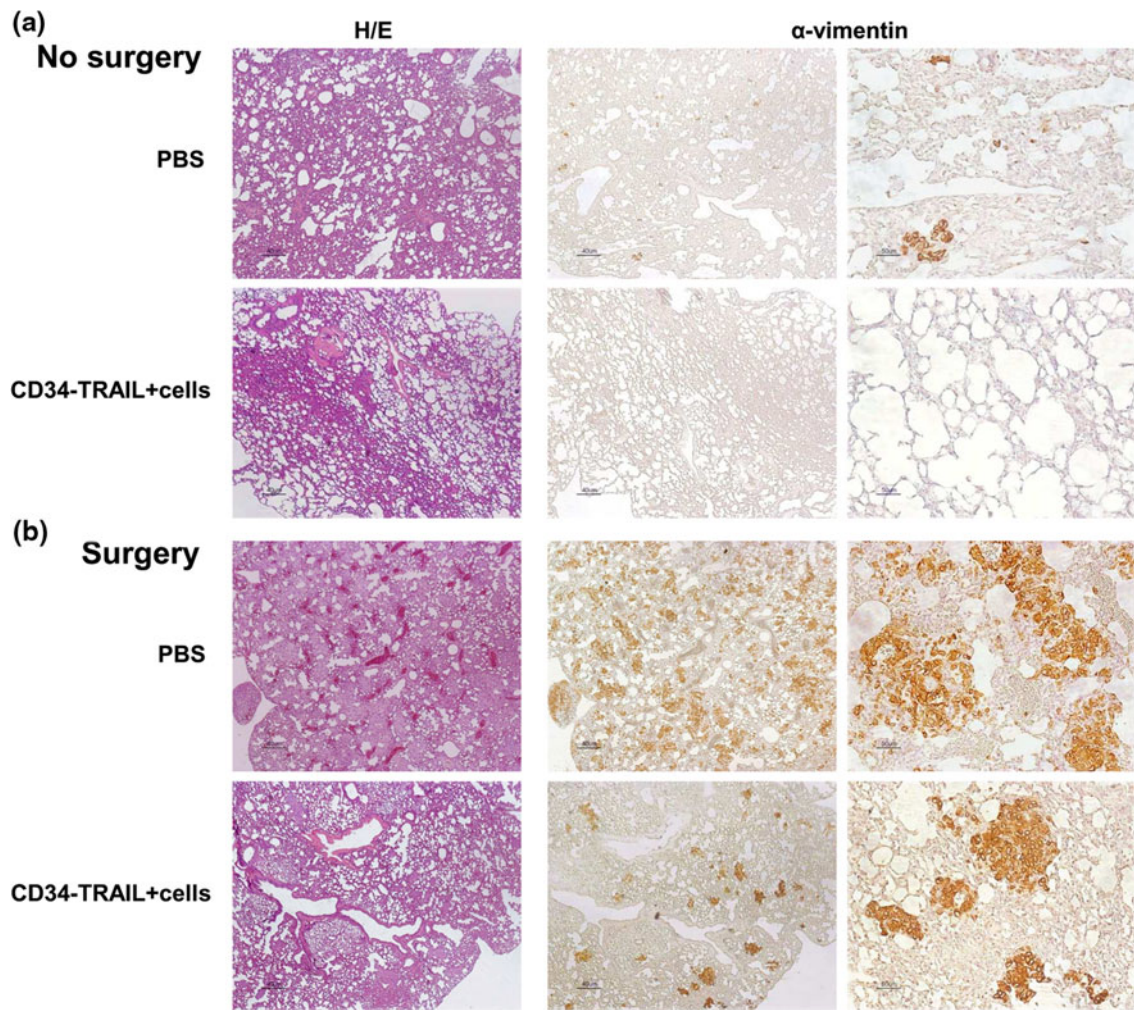
Fig. 5 Effects of CD34-TRAIL$^+$ cell treatment on lung metastases, Excised lungs from CD34-TRAIL$^+$cell- and PBS-treated mice were analyzed for the presence of metastases by hematoxylin and eosin (H/E) and immunohistochemical staining for vimentin, a mesenchymal marker highly expressed in MDA-MB-231 cells. **a** Mice killed 12 days after the last treatment (no surgery); **b** Mice killed18 days after surgical removal of the tumor (surgery). Images are of one representative mouse for each experimental group. Original magnifications, $\times$ 4; and $\times$ 20

associated with the pluripotent gene expression pattern in aggressive tumor cells and described for different tumors, including breast [34, 35]. Indeed, no significant inhibition of MDA-MB-231 tumor growth was observed in mice injected with these cells in the mammary fat-pad and treated with the anti-vascular endothelial growth factor A (VEGF-A) antibody bevacizumab (not shown).

Despite no activity of CD34-TRAIL$^+$ cells on tumor growth rate, mice treated with these cells and sacrificed when the s.c. tumor was relatively small showed no lung metastases, while lung metastases were present in all control mice bearing s.c. tumors of superimposable size. The inability of CD34-armed cells to interfere with the growth rate of s.c. tumors versus their anti-metastatic activity may be explained by their ability to induce a selective elimination among CD44$^+$/CD24$^{-/low}$ cells of

those crucial for the metastatic process, but not of those involved in the continuing growth of a subcutaneous tumor.

Further studies are needed to determine whether the inhibition of metastases by CD34-TRAIL$^+$ cells is related to their effect on stem cells present in the primary s.c. tumor or on stem cells that have already migrated to the lungs. In any case, the ability of CD34-armed cells to mediate a loss of function of stem cell metastatic activity points to the value of treatment with CD34-TRAIL$^+$ cells, suggesting their possible use in adjuvant therapy. Our results on the ability of TRAIL-expressing CD34$^+$ cells to subvert the breast cancer metastatic process are consistent with the reported significant reduction in metastatic tumor burden upon treatment with inducible TRAIL-expressing bone marrow-derived mesenchymal stem cells [36], although that analysis was

performed only in mice i.v.-injected with tumor cells, while our results were also obtained in spontaneous lung metastases models.

While the selective targeting of cancer stem cells by CD34-armed cells remains to be confirmed, the correlation between in vitro susceptibility to mTRAIL and amount of tumor stem cells, together with the CD34-TRAIL$^+$ cell-induced inhibition of the metastatic process, point to CD34-armed cell treatment as a viable approach to eradicate stem tumor cells before the onset of overt metastases.

References

1. Jin Z, El-Deiry WS (2005) Overview of cell death signaling pathways. Cancer Biol Ther 4:139–163

2. Debatin KM, Stahnke K, Fulda S (2003) Apoptosis in hematological disorders. Semin Cancer Biol 13:149–158

3. Krammer PH (2000) CD95's deadly mission in the immune system. Nature 407:789–795

4. Wiley SR, Schooley K, Smolak PJ, Din WS, Huang CP, Nicholl JK, Sutherland GR, Smith TD, Rauch C, Smith CA (1995) Identification and characterization of a new member of the TNF family that induces apoptosis. Immunity 3:673–682

5. Ashkenazi A (2008) Directing cancer cells to self-destruct with pro-apoptotic receptor agonists. Nat Rev Drug Discov 7:1001–1012

6. Carlo-Stella C, Lavazza C, Di Nicola M, Cleris L, Longoni P, Milanesi M, Magni M, Morelli D, Gloghini A, Carbone A, Gianni AM (2006) Antitumor activity of human CD34 + cells expressing membrane-bound tumor necrosis factor-related apoptosis-inducing ligand. Hum Gene Ther 17:1225–1240

7. Lavazza C, Carlo-Stella C, Di Nicola M, Longoni P, Milanesi M, Magni M, Gianni AM (2007) Highly efficient gene transfer into mobilized CD34 + hematopoietic cells using serotype-5 adenoviral vectors and BoosterExpress Reagent. Exp Hematol 35:888–897

8. Verfaillie CM (1998) Adhesion receptors as regulators of the hematopoietic process. Blood 92:2609–2612

9. Burger JA, Kipps TJ (2006) CXCR4: a key receptor in the crosstalk between tumor cells and their microenvironment. Blood 107:1761–1767

10. Jin H, Aiyer A, Su J, Borgstrom P, Stupack D, Friedlander M, Varner J (2006) A homing mechanism for bone marrow-derived progenitor cell recruitment to the neovasculature. J Clin Invest 116:652–662

11. Tavassoli M, Minguell JJ (1991) Homing of hemopoietic progenitor cells to the marrow. Proc Soc Exp Biol Med 196:367–373

12. Kaplan RN, Riba RD, Zacharoulis S, Bramley AH, Vincent L, Costa C, MacDonald DD, Jin DK, Shido K, Kerns SA, Zhu Z, Hicklin D, Wu Y, Port JL, Altorki N, Port ER, Ruggero D,

Shmelkov SV, Jensen KK, Rafii S, Lyden D (2005) VEGFR1-positive haematopoietic bone marrow progenitors initiate the pre-metastatic niche. Nature 438:820–827

13. Aboody KS, Najbauer J, Danks MK (2008) Stem and progenitor cell-mediated tumor selective gene therapy. Gene Ther 15:739–752

14. Lavazza C, Carlo-Stella C, Giacomini A, Cleris L, Righi M, Sia D, Di Nicola M, Magni M, Longoni P, Milanesi M, Francolini M, Gloghini A, Carbone A, Formelli F, Gianni AM (2010) Human CD34 + cells engineered to express membrane-bound tumor necrosis factor-related apoptosis-inducing ligand target both tumor cells and tumor vasculature. Blood 115:2231–2240

15. Kayagaki N, Yamaguchi N, Nakayama M, Kawasaki A, Akiba H, Okumura K, Yagita H (1999) Involvement of TNF-related apoptosis-inducing ligand in human CD4 + T cell-mediated cytotoxicity. J Immunol 162:2639–2647

16. (1998) United Kingdom Co-ordinating Committee on Cancer Research (UKCCCR). Guidelines for the welfare of animals in experimental neoplasia (second edition). Br J Cancer 77:1–10

17. Neve RM, Chin K, Fridlyand J, Yeh J, Baehner FL, Fevr T, Clark L, Bayani N, Coppe JP, Tong F, Speed T, Spellman PT, DeVries S, Lapuk A, Wang NJ, Kuo WL, Stilwell JL, Pinkel D, Albertson DG, Waldman FM, McCormick F, Dickson RB, Johnson MD, Lippman M, Ethier S, Gazdar A, Gray JW (2006) A collection of breast cancer cell lines for the study of functionally distinct cancer subtypes. Cancer Cell 10:515–527

18. Sieuwerts AM, Kraan J, Bolt J, van der Spoel P, Elstrodt F, Schutte M, Martens JW, Gratama JW, Sleijfer S, Foekens JA (2009) Anti-epithelial cell adhesion molecule antibodies and the detection of circulating normal-like breast tumor cells. J Natl Cancer Inst 101:61–66

19. Rahman M, Davis SR, Pumphrey JG, Bao J, Nau MM, Meltzer PS, Lipkowitz S (2009) TRAIL induces apoptosis in triple-negative breast cancer cells with a mesenchymal phenotype. Breast Cancer Res Treat 113:217–230

20. Al-Hajj M, Wicha MS, ito-Hernandez A, Morrison SJ, Clarke MF (2003) Prospective identification of tumorigenic breast cancer cells. Proc Natl Acad Sci USA 100:3983–3988

21. Prat A, Parker JS, Karginova O, Fan C, Livasy C, Herschkowitz JI, He X, Perou CM (2010) Phenotypic and molecular characterization of the claudin-low intrinsic subtype of breast cancer. Breast Cancer Res 12:R68

22. Mani SA, Guo W, Liao MJ, Eaton EN, Ayyanan A, Zhou AY, Brooks M, Reinhard F, Zhang CC, Shipitsin M, Campbell LL, Polyak K, Brisken C, Yang J, Weinberg RA (2008) The epithelial-mesenchymal transition generates cells with properties of stem cells. Cell 133:704–715

23. Tang X, Sun Z, Runne C, Madsen J, Domann F, Henry M, Lin F, Chen S (2011) A critical role of Gbetagamma in tumorigenesis and metastasis of breast cancer. J Biol Chem 286:13244–13254

24. Ehtesham M, Kabos P, Kabosova A, Neuman T, Black KL, Yu JS (2002) The use of interleukin 12-secreting neural stem cells for the treatment of intracranial glioma. Cancer Res 62:5657–5663

25. Studeny M, Marini FC, Dembinski JL, Zompetta C, Cabreira-Hansen M, Bekele BN, Champlin RE, Andreeff M (2004) Mesenchymal stem cells: potential precursors for tumor stroma and targeted-delivery vehicles for anticancer agents. J Natl Cancer Inst 96:1593–1603

26. Wei J, Blum S, Unger M, Jarmy G, Lamparter M, Geishauser A, Vlastos GA, Chan G, Fischer KD, Rattat D, Debatin KM, Hatzopoulos AK, Beltinger C (2004) Embryonic endothelial progenitor cells armed with a suicide gene target hypoxic lung metastases after intravenous delivery. Cancer Cell 5:477–488

27. Kucerova L, Altanerova V, Matuskova M, Tyciakova S, Altaner C (2007) Adipose tissue-derived human mesenchymal stem cells

mediated prodrug cancer gene therapy. Cancer Res 67: 6304–6313

28. Ganten TM, Haas TL, Sykora J, Stahl H, Sprick MR, Fas SC, Krueger A, Weigand MA, Grosse-Wilde A, Stremmel W, Krammer PH, Walczak H (2004) Enhanced caspase-8 recruitment to and activation at the DISC is critical for sensitisation of human hepatocellular carcinoma cells to TRAIL-induced apoptosis by chemotherapeutic drugs. Cell Death Differ 11(Suppl 1):S86-96

29. Keane MM, Ettenberg SA, Nau MM, Russell EK, Lipkowitz S (1999) Chemotherapy augments TRAIL-induced apoptosis in breast cell lines. Cancer Res 59:734–741

30. Singh TR, Shankar S, Chen X, Asim M, Srivastava RK (2003) Synergistic interactions of chemotherapeutic drugs and tumor necrosis factor-related apoptosis-inducing ligand/Apo-2 ligand on apoptosis and on regression of breast carcinoma in vivo. Cancer Res 63:5390–5400

31. Ganten TM, Koschny R, Haas TL, Sykora J, Li-Weber M, Herzer K, Walczak H (2005) Proteasome inhibition sensitizes hepatocellular carcinoma cells, but not human hepatocytes, to TRAIL. Hepatology 42:588–597

32. Buchsbaum DJ, Zhou T, Grizzle WE, Oliver PG, Hammond CJ, Zhang S, Carpenter M, LoBuglio AF (2003) Antitumor efficacy of TRA-8 anti-DR5 monoclonal antibody alone or in combination with chemotherapy and/or radiation therapy in a human breast cancer model. Clin Cancer Res 9:3731–3741

33. Li M, Knight DA, Smyth MJ, Stewart TJ (2012) Sensitivity of a novel model of mammary cancer stem cell-like cells to TNF-related death pathways. Cancer Immunol Immunother 61(8): 1255–1268

34. Liu TJ, Sun BC, Zhao XL, Zhao XM, Sun T, Gu Q, Yao Z, Dong XY, Zhao N, Liu N (2012) CD133(+) cells with cancer stem cell characteristics associates with vasculogenic mimicry in triple-negative breast cancer. Oncogene. doi:10.1038/onc.2012.85

35. Ricci-Vitiani L, Pallini R, Biffoni M, Todaro M, Invernici G, Cenci T, Maira G, Parati EA, Stassi G, Larocca LM, De MR (2010) Tumour vascularization via endothelial differentiation of glioblastoma stem-like cells. Nature 468:824–828

36. Loebinger MR, Eddaoudi A, Davies D, Janes SM (2009) Mesenchymal stem cell delivery of TRAIL can eliminate metastatic cancer. Cancer Res 69:4134–4142